

Predictive Coding-based Deep Neural Network Fine-tuning for Computationally Efficient Domain Adaptation

Matteo Cardoni^[0000–0002–2759–5310] and
Sam Leroux^[0000–0003–3792–5026]

IDLab, Department of Information and Technology, Ghent University—imec,
9052 Ghent, Belgium
`matteo.cardoni@ugent.be` (Corresponding author),
`sam.leroux@ugent.be`

Abstract. As deep neural networks are increasingly deployed in dynamic, real-world environments, relying on a single static model is often insufficient. Changes in input data distributions caused by sensor drift or lighting variations necessitate continual model adaptation. In this paper, we propose a hybrid training methodology that enables efficient on-device domain adaptation by combining the strengths of Backpropagation and Predictive Coding. The method begins with a deep neural network trained offline using Backpropagation to achieve high initial performance. Subsequently, Predictive Coding is employed for online adaptation, allowing the model to recover accuracy lost due to shifts in the input data distribution. This approach leverages the robustness of Backpropagation for initial representation learning and the computational efficiency of Predictive Coding for continual learning, making it particularly well-suited for resource-constrained edge devices or future neuromorphic accelerators. Experimental results on the MNIST and CIFAR-10 datasets demonstrate that this hybrid strategy enables effective adaptation with a reduced computational overhead, offering a promising solution for maintaining model performance in dynamic environments.

Keywords: Predictive Coding · on-device learning · domain adaptation

1 Introduction

The Backpropagation (BP) algorithm [1] is currently the predominant approach for training deep neural network architectures. It is, however, not without its limitations. BP requires the computation and transmission of global error signals which can be computationally intensive, apart from being biologically implausible. This has sparked interest in alternative training techniques such as those based on Predictive Coding (PC) [2–4]. While most of the works in this area are grounded in theoretical neuroscience, PC is also promising from an engineering point of view as it provides a much more efficient hardware-friendly training

procedure for neuromorphic systems. Unlike BP, PC relies on local computations and error-driven updates that align well with the distributed, event-driven nature of neuromorphic architectures. This makes it a compelling candidate for developing scalable, low-power learning algorithms suitable for real-time applications on energy-constrained edge devices [5].

Despite the progress made in recent years, models trained using PC still fall short of the accuracy levels achieved by those trained with BP, particularly when applied to deeper architectures and more complex datasets [6, 7]. In this paper, we propose a novel hybrid approach that combines the strengths of both algorithms. As illustrated in Figure 1, we introduce a two-stage training and deployment pipeline. In the first stage, a model is trained offline using BP on high-performance cloud infrastructure with virtually unlimited computational resources. This allows us to reach an accuracy level that would be currently impossible to achieve using PC alone.

The trained model is then deployed on a resource-constrained edge device such as a wearable or sensor node. Over time, shifts in the input data distribution due to sensor drift, environmental changes, or user behavior may degrade model performance, necessitating continual adaptation. To address this, we propose using PC as a lightweight, local learning mechanism that allows efficient on-device updates, without the need for expensive BP or communication with the cloud.

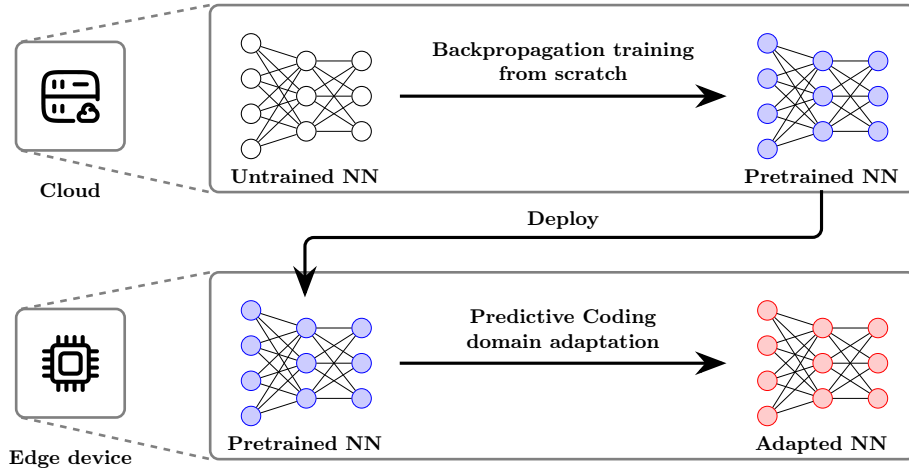


Fig. 1: Schematic overview of our proposed approach. After training a model offline using Backpropagation (BP), we employ Predictive Coding (PC) for on-device domain adaptation.

The remainder of this paper is structured as follows: we provide an overview of the related work in Section 2 and describe our experimental setup and results

in Section 3. We conclude in Section 4 and give some pointers for future research directions in this area.

2 Related work

This section provides a basic overview of Backpropagation and Predictive Coding for neural network training. We refer to [8] for a more in-depth tutorial.

2.1 Neural networks

A feedforward neural network (FNN) consists of a stack of L layers, indexed as $\{l_0, l_1, \dots, l_L\}$, with each layer defined by its weight matrix θ_l . Each layer l computes an activity a_l transforming its input activity a_{l-1} as follows:

$$a_l = f(a_{l-1}, \theta_l) \quad (1)$$

This transformation depends on the type of layer (e.g. fully connected, convolutional, ...) and typically includes a non-linear activity. Setting the activation a_0 to a datapoint x , the neural network performs a function NN: $X \rightarrow Y$:

$$\text{NN}(x) = (l_L \circ l_{L-1} \circ l_{L-2} \circ \dots \circ l_1)(x) \quad (2)$$

The weights of the model θ are initialized randomly and tuned using a training procedure to achieve the desired behavior.

2.2 Backpropagation

Backpropagation (BP) is the most widely used technique for training neural networks. It aims to minimize a global loss function \mathcal{L} that quantifies the discrepancy between the network's output and the desired target output. Common loss functions include Mean Squared Error (MSE) for regression tasks and Cross-entropy loss for classification tasks. The BP algorithm is able to calculate a suitable set of weights $\hat{\theta}$ numerically using gradient descent:

$$\hat{\theta} = \underset{\theta}{\operatorname{argmin}} \mathcal{L}(\theta) \quad (3)$$

In BP, the error of each layer is the gradient of the loss with respect to the activation of that layer. Because this depends on the gradients of subsequent layers, this backward computation must proceed sequentially from the output layer to the input layer. As a result, the gradient computation across layers is inherently sequential.

2.3 Predictive Coding

Predictive Coding (PC) training for deep neural network architectures differs fundamentally from Backpropagation (BP) in that it only uses local information to perform weight updates. During training, an input sample x is clamped to the first layer activity (a_0) and the last layer (a_L) is clamped to the desired output y . We then repeat a two-step training procedure:

1. **Inference step:** In this step, the weights θ_l are held fixed. Each layer predicts the activity of the next layer:

$$\mu_l = f(a_{l-1}, \theta_l) \quad (4)$$

The predictions μ_L are then used to calculate a layer-wise prediction error that measures the discrepancy between the actual and predicted activity:

$$\varepsilon_l = a_l - \mu_l \quad (5)$$

Unlike during BP-based training, the actual activity of the layers is not obtained by passing the input through the model, as in Equation 1. It is, instead, obtained by minimizing the energy function, which is the sum of the layer-wise prediction errors:

$$E(a, \theta) = \frac{1}{2} \sum_l (\varepsilon_l)^2 \quad (6)$$

The updated values of the activities are obtained as the minimum of the energy function:

$$\hat{a}_l = \underset{a_l}{\operatorname{argmin}} E(a, \theta) \quad (7)$$

The \hat{a}_l are typically obtained via local gradient descent of Equation 6, calculating the update of a_l as:

$$\Delta a_l = -\gamma \frac{\partial E}{\partial a_l} = -\gamma \left(\varepsilon_l - (\theta_l)^T \varepsilon_{l+1} \odot f'(\theta_l a_l) \right), \quad (8)$$

with γ being the *inference rate*: a step size required by the gradient descent. This step infers the suitable activity values for the different layers, given the clamped input and target values and is typically performed by running gradient descent for a fixed number of iterations.

It is to be noted that the dependency of Δa_l from ε_l and ε_{l+1} allows ε_L , the error between the classification layer activity a_L and the label y , to be propagated from the output layer L to the input. Moreover, this computation can be layer-wise parallelized.

2. **Weight update step:** The activities, after being updated, are now held fixed, and the weights are updated to further reduce the energy function from Equation 6. The updated weights values are obtained as the minimum of the energy function:

$$\hat{\theta}_l = \underset{\theta_l}{\operatorname{argmin}} E(\hat{a}, \theta) \quad (9)$$

The updates of θ_l are obtained via local gradient descent:

$$\Delta\theta_l = -\alpha \frac{\partial E}{\partial \theta_l} = \alpha \varepsilon_{l+1} \odot f'(\theta_l \hat{a}_l) (\hat{a}_l)^T, \quad (10)$$

with α being the weights learning rate. This computation too can be layer-wise parallelized.

2.4 Backpropagation-Predictive Coding equivalence at test time

At test time, the activity of each layer in the Predictive Coding Network model, including the last layer, can be obtained by clamping the lowest layer to the input data and by computing updates of the activity by repeating the inference procedure. However, with the output unclamped, this can also be computed in a single pass by simply performing the forward pass of a normal neural network [8]. This observation that models trained using Backpropagation and Predictive Coding are equivalent at test time is what motivated this work as it allows switching between both training algorithms while maintaining a compatible model.

2.5 Applications of Predictive Coding

Predictive Coding has seen growing application in recent years across a range of increasingly complex tasks. Initial studies focused on classification, associative memory, and denoising using Multi-Layer Perceptron (MLP) architectures [7, 9, 10]. Building on these foundations, more recent work has extended PC to convolutional neural networks (CNNs) for higher-level visual tasks. For example, [11, 12] introduced recurrent variants of PC networks that achieved classification performance comparable to Backpropagation on the CIFAR-10 dataset, and promising, though less competitive, results on ImageNet. Furthermore, [7] systematically benchmarked PC training in both MLPs and CNNs for classification and associative memory tasks. This work also introduced a JAX-based implementation framework [13], which forms the basis for the PC models used in our work.

2.6 Domain adaptation and on-device learning

Classical artificial intelligence approaches typically assume that the training and test data are drawn from the same underlying distribution. However, this assumption often breaks down in real-world applications, particularly when deploying pretrained neural networks on devices that process data from dynamic, non-stationary environments [14, 15]. Domain adaptation seeks to address this mismatch by adapting models trained on a source domain to perform well on a target domain with a different marginal data distribution.

Domain adaptation is particularly important in scenarios where a model is deployed on a physical device operating in a specific environment. These edge

devices typically have limited computational and energy resources, which preclude the use of large, resource-intensive models. Instead, a lightweight, location-specific model, adapted to the unique characteristics of the local sensor or environment, can achieve performance comparable to that of a larger, general-purpose model, while being significantly more energy-efficient and responsive [16]. While it is possible to perform the domain adaptation remotely, on cloud infrastructure, a full on-device approach is favorable in terms of privacy, communication overhead and system cost [17]. Novel algorithms that can perform this training more efficiently are therefore of high value for advancing adaptive intelligence at the edge. To the best of our knowledge, this work is the first to consider Predictive Coding for on-device domain adaptation.

3 Experiments and results

3.1 Experimental setup

We report results on the well-known MNIST [18] and CIFAR-10 [19] image classification benchmarks. Following the setup in [7], we use a three-layer fully connected neural network for MNIST, and a series of convolutional architectures inspired by the VGG family [20] for CIFAR-10. Full model specifications and training hyperparameters are provided in the Appendix.

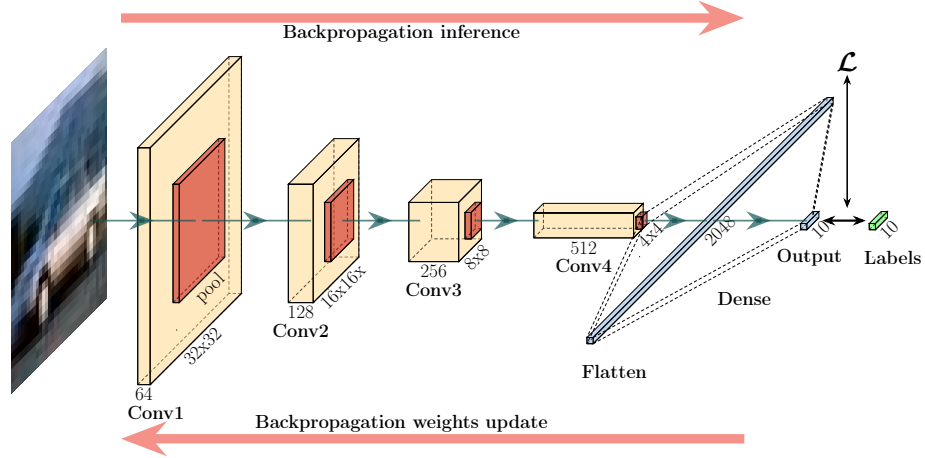
All experiments were implemented using JAX [13]. Models trained with Backpropagation (BP), along with their training procedures, were implemented in Equinox [21]. Instead, models trained with Predictive Coding (PC), along with their training procedures, were implemented in the PCX library [7], which generalizes the gradients computation from Equations 8 and 10 by means of the JAX automatic differentiation.

Each model was initially trained from scratch using BP on the original dataset (the details of these trainings are reported in the Appendix). To simulate domain shifts, the training and test images were then transformed in three different ways, for three different scenarios:

- Inversion (180 degrees rotation).
- Clockwise rotation of 20 degrees.
- Addition of random uniform noise in the range of $[-0.05, 0.05]$ per channel (while the pixel values are in the range $[0, 1]$).

We evaluated the performance of both BP and PC in adapting the pretrained models to this transformed data, assessing their ability to recover lost accuracy under this input perturbation. The domain adaptation took place retraining on the entire training dataset after applying the corresponding transformation. Figure 2 visualizes the procedure, for the case where a VGG5 model (see Appendix for details) is used for training and domain adaptation on the CIFAR-10 dataset. All experiments were conducted on a cloud infrastructure.

1. Train using Backpropagation for original dataset



2. Fine-tune using Predictive Coding for domain-shifted dataset

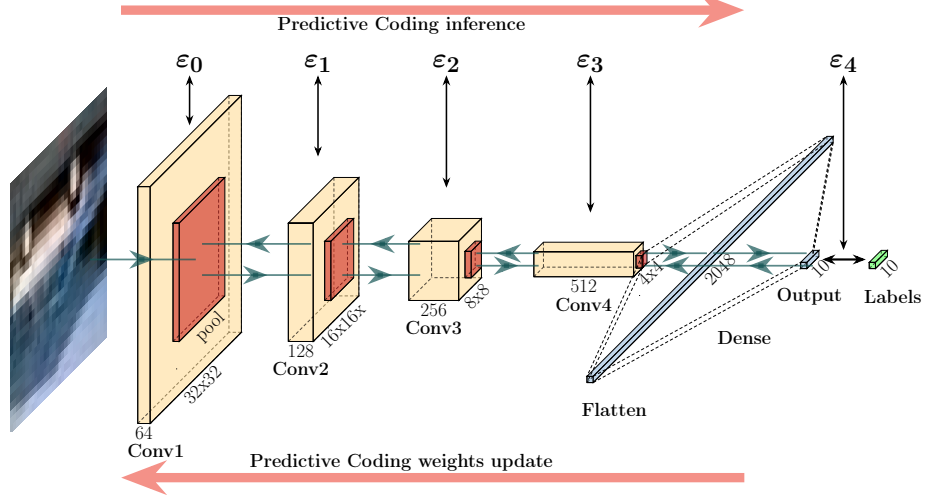


Fig. 2: Experiment workflow, including the initial training of a VGG5 (see Appendix for the architecture detail) for the CIFAR-10 dataset in its original version. The same Neural Network is subsequently retrained with a domain-shifted version of the dataset. In this case, an image inversion (180 degrees rotation) has been applied to all the images. Opposite to the Backpropagation (BP), Predictive Coding (PC) training is based on layer-wise errors ϵ_l , that allows to compute local gradient of the weights, as in Equation 10

3.2 Results

Table 1 reports the average training time per epoch for both Backpropagation (BP) and Predictive Coding (PC), measured on a GeForce GTX 1080 Ti GPU. To obtain an accurate comparison, only the training time, after data loading, has been measured. Since the data transformations simulate domain shifts in data sampled by a sensor, also the data transformation has been excluded from the measurement time.

The results show that for the convolutional models, PC achieves a substantial speed advantage, with an average training time that is only 52% of that required by BP. In contrast, for the MLP model, the PC training times are on average 56% higher, likely due to the simplicity of the architecture, which limits the potential gains in efficiency from PC.

Table 1: Wall-clock time per epoch (in seconds) for both Backpropagation (BP) and Predictive Coding (PC), averaged over 10 epochs for the MLP model and over 100 epochs for the VGG models. Values are reported as mean \pm standard deviation. For the CNN-based architectures, PC is on average twice as fast.

Dataset	Model	BP	PC
MNIST	MLP	1.88 ± 0.29	2.93 ± 3.17
	VGG5	9.48 ± 0.28	4.34 ± 1.48
CIFAR10	VGG7	10.48 ± 0.88	5.16 ± 2.06
	VGG9	8.48 ± 0.58	5.43 ± 1.79

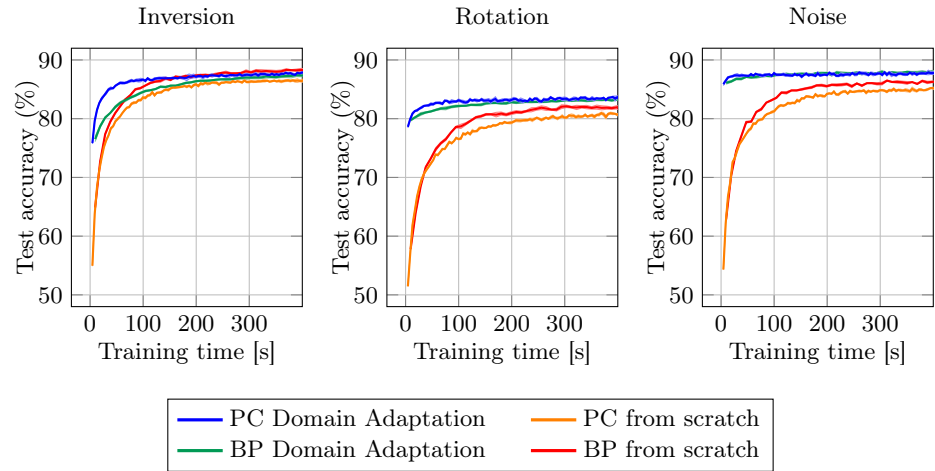
Although these results demonstrate that PC can reach a higher training throughput compared to BP, this does not necessarily mean that it results in faster training (i.e. performance increase over time), since accuracy gains per epoch vary across models and under different domain shifts. To investigate this, Figure 3 shows the models test accuracy on the domain shifted input data as a function of the training time. We compare our PC-based domain adaptation approach with a BP-based approach. As a baseline, we also include the performance for a PC and a BP model, trained from scratch on the domain-shifted data. All training details can be found in the Appendix.

The graphs show both the mean accuracies (middle lines) and standard deviations (color-filled areas) resulting from 5 different executions. In some of the plots the standard deviation is hardly noticeable, due to the small variance over different runs.

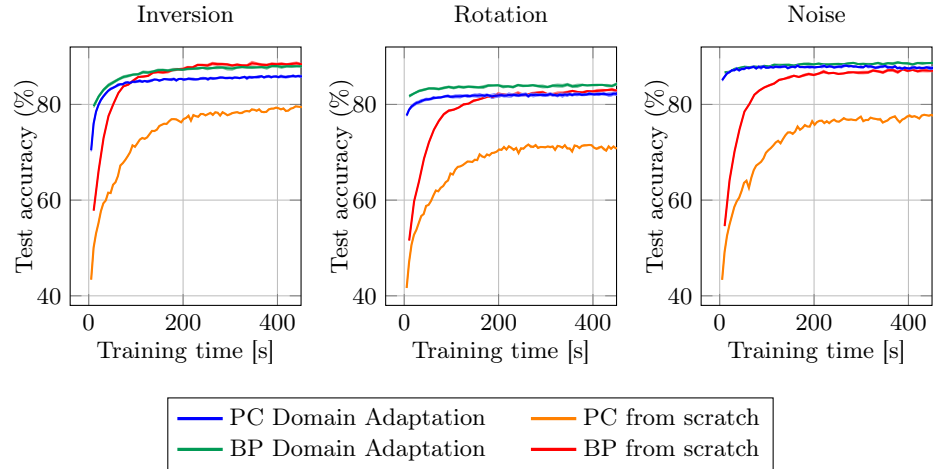
For the inverted data, the BP training from scratch baseline consistently obtains the highest accuracy. For the VGG5 model, our proposed PC-based domain adaptation achieves a similar accuracy ($87.7\% \pm 0.2\%$ compared to $88.2\% \pm 0.2\%$). The VGG5 model almost reaches the accuracy obtained by the BP from scratch training, but with a much faster training, outperforming the BP-based adaptation ($87.2\% \pm 0.3\%$) and PC-based training from scratch ($86.5\% \pm 0.1\%$).

These values correspond to the peak accuracy observed within 350 seconds of training. The two other domain shifts proved to be more challenging, resulting in lower accuracies overall. Here, all models benefit from pretraining combined with domain adaptation. For the VGG5 model, PC-based domain adaptation matches or surpasses the accuracy obtained with BP domain adaptation for rotated and noisy data, while it obtains a slightly lower accuracy on the VGG7 model.

The models trained from scratch using PC obtain significantly lower accuracies compared to their counterparts trained using BP. The performance of PC-based algorithms decreases as model depth increases, as is evident for the deeper VGG9 model. This aligns with previous observations that PC struggles when training



(a) VGG5



(b) VGG7

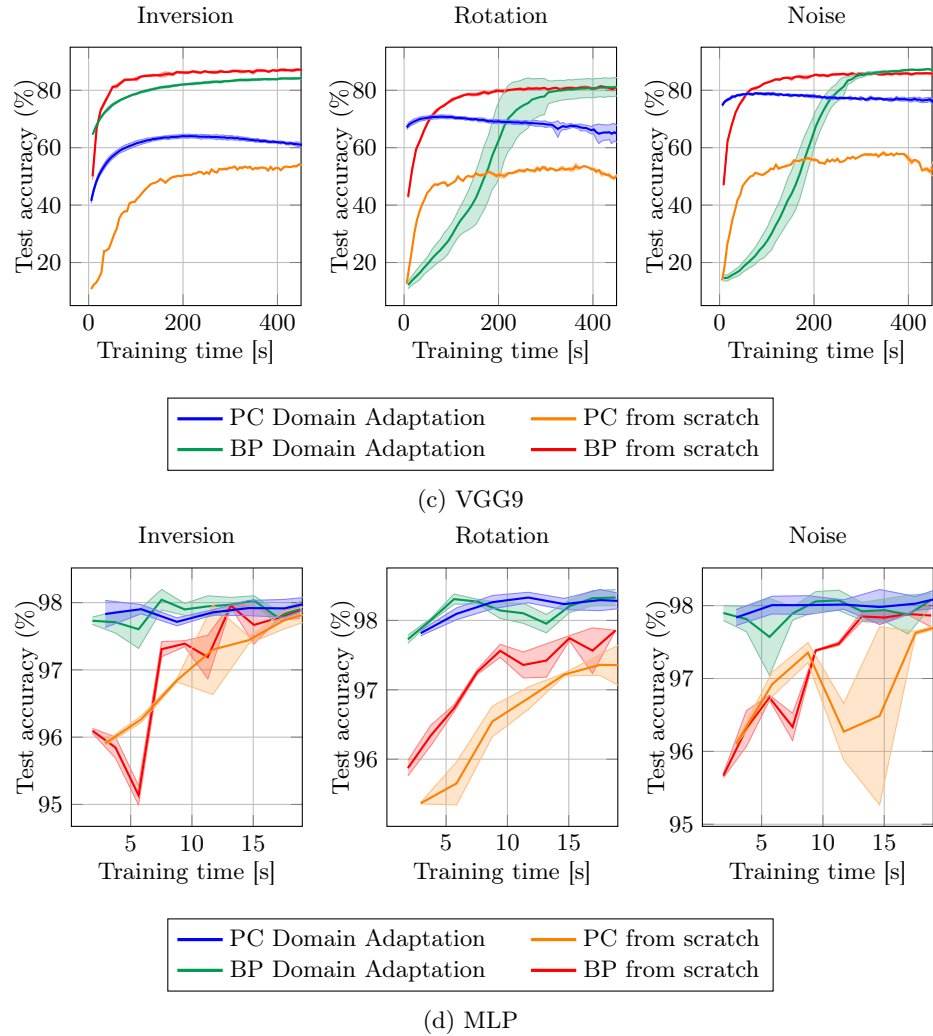


Fig. 3: Model Accuracy as a function of training time for models trained from scratch and domain-adapted using Backpropagation (BP) and Predictive Coding (PC). Trainings were performed, for each model, respectively with inverted, rotated and noisy data (Section 3.1). The plots highlight the validity brought by the proposed technique, especially for the VGG5 model. The transparent areas represent the accuracy standard deviation over five runs.

deep architectures [6, 7], while it can outperform BP for more shallow architectures [7]. The BP-based domain adaptation for VGG9 delivers lower performances with respect to the BP-based domain adaptation of the other models, highlighting that domain adaptation may in general be more difficult for deeper

models, regardless of the training technique. For the easier MNIST dataset with a simple three layer MLP model, both the PC and BP domain adaptation prove to be beneficial, providing equally accurate models. Both approaches outperform training a model from scratch.

4 Conclusion and future work

Our experiments demonstrate that Predictive Coding (PC) is an efficient algorithm for on-device domain adaptation of models initially pretrained with Back-propagation (BP). We showed that models trained with BP can effectively leverage PC-based finetuning on a domain-shifted variant of the same dataset—in our case, MNIST and CIFAR-10. This opens up new avenues of research into computationally efficient domain adaptation techniques using PC. This could prove especially efficient when implemented on neuromorphic hardware [22].

Future work will extend this study by evaluating training times on embedded platforms, including neuromorphic hardware. We also aim to scale our approach to deeper neural network architectures. While the domain adaptation procedure was completely supervised in this work, this might not be feasible in real-world environments. More research into unsupervised or self-supervised approaches in combination with PC is therefore a highly interesting research direction.

Acknowledgments

This research was supported by funding from the Flemish Government under the “Onderzoeksprogramma Artificiële Intelligentie (AI) Vlaanderen” program.

References

1. David E Rumelhart, Geoffrey E Hinton, and Ronald J Williams. Learning representations by back-propagating errors. *nature*, 323(6088):533–536, 1986.
2. Rajesh Rao and Dana Ballard. Predictive coding in the visual cortex: a functional interpretation of some extra-classical receptive-field effects. *Nature neuroscience*, 2:79–87, 02 1999.
3. Karl Friston. A theory of cortical responses. *Philosophical transactions of the Royal Society of London. Series B, Biological sciences*, 360:815–36, 04 2005.
4. Karl Friston and Stefan Kiebel. Predictive coding under the free-energy principle. *Philosophical transactions of the Royal Society of London. Series B, Biological sciences*, 364:1211–21, 05 2009.
5. Beren Millidge, Tommaso Salvatori, Yuhang Song, Rafal Bogacz, and Thomas Lukasiewicz. Predictive coding: Towards a future of deep learning beyond back-propagation? arXiv preprint arXiv:2202.09467, 2022.
6. Cédric Goemaere, Gaspard Oliviers, Rafal Bogacz, and Thomas Demeester. Error optimization: Overcoming exponential signal decay in deep predictive coding networks. arXiv preprint arXiv:2505.20137, 2025.

7. Luca Pinchetti, Chang Qi, Oleh Lokshyn, Gaspard Olivers, Cornelius Emde, Mufeng Tang, Amine M'Charrak, Simon Frieder, Bayar Menzat, Rafal Bogacz, Thomas Lukasiewicz, and Tommaso Salvatori. Benchmarking predictive coding networks – made simple. arXiv preprint arXiv:2407.01163, 2025.
8. Björn van Zwol, Ro Jefferson, and Egon L. van den Broek. Predictive coding networks and inference learning: Tutorial and survey. arXiv preprint arXiv:2407.04117, 2024.
9. James C. R. Whittington and Rafal Bogacz. An approximation of the error back-propagation algorithm in a predictive coding network with local hebbian synaptic plasticity. *Neural Computation*, 29(5):1229–1262, 05 2017.
10. Wei Sun and Jeff Orchard. A predictive-coding network that is both discriminative and generative. *Neural Computation*, 32:1836–1862, 2020.
11. Haiguang Wen, Kuan Han, Junxing Shi, Yizhen Zhang, Eugenio Culurciello, and Zhongming Liu. Deep predictive coding network for object recognition. arXiv preprint arXiv:1802.04762, 2018.
12. Kuan Han, Haiguang Wen, Yizhen Zhang, Di Fu, Eugenio Culurciello, and Zhongming Liu. Deep predictive coding network with local recurrent processing for object recognition. arXiv preprint arXiv:1805.07526, 2018.
13. James Bradbury, Roy Frostig, Peter Hawkins, Matthew James Johnson, Chris Leary, Dougal Maclaurin, George Necula, Adam Paszke, Jake VanderPlas, Skye Wanderman-Milne, and Qiao Zhang. JAX: composable transformations of Python+NumPy programs. <http://github.com/google/jax>, 2018.
14. Abolfazl Farahani, Sahar Voghoei, Khaled Rasheed, and Hamid R. Arabnia. A brief review of domain adaptation. In Robert Stahlbock, Gary M. Weiss, Mahmoud Abou-Nasr, Cheng-Ying Yang, Hamid R. Arabnia, and Leonidas Deligiannidis, editors, *Advances in Data Science and Information Engineering*, pages 877–894, Cham, 2021. Springer International Publishing.
15. Shiliang Sun, Honglei Shi, and Yuanbin Wu. A survey of multi-source domain adaptation. *Information Fusion*, 24:84–92, 2015.
16. Sam Leroux, Bo Li, and Pieter Simoons. Automated training of location-specific edge models for traffic counting. *Computers and Electrical Engineering*, 99:107763, 2022.
17. Tianming Zhao, Yucheng Xie, Yan Wang, Jerry Cheng, Xiaonan Guo, Bin Hu, and Yingying Chen. A survey of deep learning on mobile devices: Applications, optimizations, challenges, and research opportunities. *Proceedings of the IEEE*, 110(3):334–354, 2022.
18. Li Deng. The mnist database of handwritten digit images for machine learning research [best of the web]. *IEEE Signal Processing Magazine*, 29(6):141–142, 2012.
19. Alex Krizhevsky. Learning multiple layers of features from tiny images. pages 32–33, 2009.
20. Karen Simonyan and Andrew Zisserman. Very deep convolutional networks for large-scale image recognition. arXiv preprint arXiv:1409.1556, 2015.
21. Patrick Kidger and Cristian Garcia. Equinox: neural networks in JAX via callable PyTrees and filtered transformations. *Differentiable Programming workshop at Neural Information Processing Systems 2021*, 2021.
22. J. Ajayan, D. Nirmal, Binola K Jebalin I.V, and S. Sreejith. Advances in neuromorphic devices for the hardware implementation of neuromorphic computing systems for future artificial intelligence applications: A critical review. *Microelectronics Journal*, 130:105634, 2022.

23. Luca Pinchetti, Tommaso Salvatori, Yordan Yordanov, Beren Millidge, Yuhang Song, and Thomas Lukasiewicz. Predictive coding beyond gaussian distributions. In *Proceedings of the 36th International Conference on Neural Information Processing Systems*, NIPS '22, Red Hook, NY, USA, 2022. Curran Associates Inc.

Appendix

Table 2 reports the MLP architecture that was used in this study, while Table 3 describes the VGG-inspired architectures [20]. Both the MLP and VGG architectures follow the setup from [7].

Table 2: Summary of the MLP model for MNIST classification

MLP
Dense(784, 512)
Leaky ReLU
Dense(512, 512)
Leaky ReLU
Dense(512, 10)

Table 3: Summary of The VGG5, VGG7, and VGG9 models, inspired from [20]. The notation Conv $\langle n \rangle$ _ $\langle m \rangle$ stands for a 2D convolutional layer with a kernel of size $n \times n$ and m channels. All Convolutional layers are followed by a GELU non-linear activation. All Max Pooling layers have a size of 2×2 and a stride of 2×2 .

VGG5	VGG7	VGG9
Conv3-128 (Pad (1, 1)) Max Pool	Conv3-128 (Pad (1, 1)) Max Pool	Conv3-128 (Pad (1, 1)) Max Pool
Conv3-256 (Pad (1, 1)) Max Pool	Conv3-128 (Pad (1, 1))	Conv3-128 (Pad (1, 1)) Max Pool
Conv3-512 (Pad (1, 1)) Max Pool	Conv3-256 (Pad (1, 1))	Conv3-256 (Pad (1, 1)) Max Pool
Conv3-512 (Pad (1, 1)) Max Pool	Conv3-256	Conv3-256 (Pad (1, 1)) Max Pool
-	Conv3-512 (Pad (1, 1)) Max Pool	Conv3-512 (Pad (1, 1))
-	Conv3-512	Conv3-512 (Pad (1, 1)) Max Pool
-	-	Conv3-512 (Pad (1, 1))
-	-	Conv3-512 (Pad (1, 1))
Dense(2048, 10)	Dense(512,10)	Dense(512, 10)

Tables 4a, 4b, and 4c describe the hyperparameters that were used to obtain the results from Figure 3.

Using the design space search from [7] as a starting point:

- Both Squared Error (SE) and Cross Entropy (CE) were used as loss function, also in Predictive Coding(PC)-based training. In fact, the energy function can be adapted, as explained in [23].
- AdamW (Adam with weight decay regularization) was used as weights optimizer.
- SGD with momentum was used as predictions optimizer (for the PC-based trainings).
- All the weights learning rate was scheduled with a linear warmup followed by cosine decay.

However, unlike in [7], the number of PC inference steps (Subsection 2.3) was kept at 4 for all CNN models. This choice was taken to obtain a training time per epoch that is, for each model, approximately half the time per epoch of the Backpropagation (BP) training counterpart. All PC trainings were performed with Forward Initialization, which is widely used to accelerate the predictions optimization [6]. This initialization technique implies that for each training batch a first forward pass (BP-like) is performed, as in Equation 1. After the forward pass, the predictions μ_l for are initialized as the activities a_l , for each layer apart from the last one, for which the labels y are used. After this step, the training takes place as in Subsection 2.3.

Figure 4 displays the test accuracy per training time, obtained with the models from Table 2 and Table 3 respectively, training them with BP on original data (i.e. not subject to domain shift). The weights obtained from this models were used as starting point for both the PC and BP-based domain adaptation techniques.

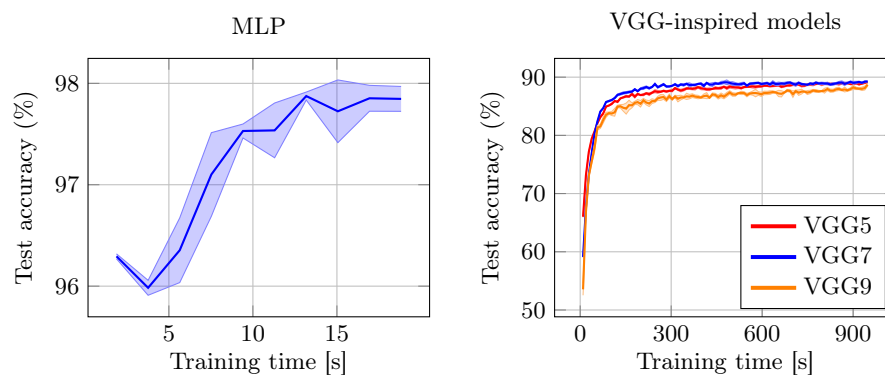


Fig. 4: Test accuracy per training time of the MLP (Table 2) and the VGG-inspired models (Table 3), training with Backpropagation (BP) on original data.

Table 4: Models training hyperparameters corresponding to each specific training technique: training from scratch and domain adaptation performed both with Backpropagation (BP) and Predictive Coding (PC). The training was performed on data subject to different domain shifts: inversion, rotation, and noise addition (see Subsection 3.1 for details). AdamW was used as weights optimizer, while SGD with momentum was used as predictions optimizer.

(a) Inverted images

	Model	Loss	θ_{lr}^*	Weight decay	γ^\dagger	m^\ddagger	Inference steps
BP from scratch	VGG5	SE	$2.5e^{-4}$	$3e^{-4}$	-	-	-
	VGG7	SE	$2.5e^{-4}$	$2e^{-4}$			
	VGG9	CE	$5e^{-4}$	$3e^{-4}$			
	MLP	CE	$1e^{-3}$	$1e^{-4}$			
BP domain adaptation	VGG5	SE	$1e^{-3}$	$2e^{-4}$	-	-	-
	VGG7	CE	$1e^{-3}$	$2e^{-4}$			
	VGG9	CE	$1e^{-3}$	$3e^{-4}$			
	MLP	CE	$1e^{-3}$	$1e^{-4}$			
PC from scratch	VGG5	SE	$1e^{-4}$	$1e^{-4}$	$2.5e^{-2}$	0.1	4
	VGG7	CE	$1e^{-4}$	$1e^{-4}$	$2.5e^{-2}$	0.1	4
	VGG9	SE	$1e^{-3}$	$1e^{-4}$	$1e^{-4}$	0.1	4
	MLP	CE	$1e^{-3}$	$1e^{-4}$	$1e^{-3}$	0.1	13
PC domain adaptation	VGG5	CE	$1e^{-4}$	$1e^{-4}$	$1e^{-2}$	0.1	4
	VGG7	CE	$1e^{-4}$	$1e^{-4}$	$1e^{-2}$	0.5	4
	VGG9	CE	$1e^{-4}$	$1e^{-4}$	$1e^{-3}$	0.1	4
	MLP	CE	$1e^{-3}$	$1e^{-4}$	$1e^{-3}$	0.1	13

* Weights learning rate.

† Inference rate.

‡ SGD optimizer momentum.

(b) Rotated images

	Model	Loss	θ_{lr}^*	Weight decay	γ^\dagger	m^\ddagger	Inference steps
BP from scratch	VGG5	SE	$2.5e^{-4}$	$2e^{-4}$			
	VGG7	SE	$2.5e^{-4}$	$3e^{-4}$			
	VGG9	SE	$5e^{-4}$	$2e^{-4}$	-	-	-
	MLP	CE	$1e^{-3}$	$1e^{-4}$			
BP domain adaptation	VGG5	SE	$5e^{-4}$	$1e^{-4}$			
	VGG7	CE	$1e^{-3}$	$1e^{-4}$			
	VGG9	SE	$1e^{-3}$	$3e^{-4}$	-	-	-
	MLP	CE	$1e^{-3}$	$1e^{-4}$			
PC from scratch	VGG5	SE	$1e^{-4}$	$1e^{-4}$	$2.5e^{-2}$	0.5	4
	VGG7	CE	$1e^{-4}$	$1e^{-4}$	$2.5e^{-2}$	0.1	4
	VGG9	SE	$1e^{-4}$	$1e^{-4}$	$1e^{-2}$	0.1	4
	MLP	CE	$1e^{-3}$	$1e^{-4}$	$1e^{-3}$	0.1	13
PC domain adaptation	VGG5	CE	$1e^{-4}$	$1e^{-4}$	$1e^{-2}$	0.1	4
	VGG7	CE	$1e^{-4}$	$1e^{-4}$	$1e^{-2}$	0.1	4
	VGG9	CE	$1e^{-4}$	$1e^{-4}$	$1e^{-2}$	0.1	4
	MLP	CE	$1e^{-3}$	$1e^{-4}$	$1e^{-3}$	0.1	13

* Weights learning rate.

† Inference rate.

‡ SGD optimizer momentum.

(c) Noisy images

	Model	Loss	θ_{lr}^*	Weight decay	γ^\dagger	m^\ddagger	Inference steps
BP from scratch	VGG5	SE	$2.5e^{-4}$	$1e^{-4}$	-	-	-
	VGG7	SE	$2.5e^{-4}$	$1e^{-4}$			
	VGG9	SE	$2.5e^{-4}$	$1e^{-4}$			
	MLP	CE	$1e^{-3}$	$1e^{-4}$			
BP domain adaptation	VGG5	CE	$2.5e^{-4}$	$3e^{-4}$	-	-	-
	VGG7	CE	$1e^{-4}$	$2e^{-4}$			
	VGG9	SE	$5e^{-4}$	$1e^{-4}$			
	MLP	CE	$1e^{-3}$	$1e^{-4}$			
PC from scratch	VGG5	SE	$1e^{-4}$	$1e^{-4}$	$2.5e^{-2}$	0.5	4
	VGG7	CE	$1e^{-4}$	$1e^{-4}$	$2.5e^{-2}$	0.1	4
	VGG9	SE	$1e^{-4}$	$1e^{-4}$	$1e^{-2}$	0.1	4
	MLP	CE	$1e^{-3}$	$1e^{-4}$	$1e^{-3}$	0.1	13
PC domain adaptation	VGG5	CE	$1e^{-4}$	$1e^{-4}$	$1e^{-2}$	0.5	4
	VGG7	CE	$1e^{-4}$	$1e^{-4}$	$2.5e^{-2}$	0.5	4
	VGG9	CE	$1e^{-4}$	$1e^{-4}$	$1e^{-2}$	0.1	4
	MLP	CE	$1e^{-3}$	$1e^{-4}$	$1e^{-3}$	0.1	13

* Weights learning rate.

† Inference rate.

‡ SGD optimizer momentum.

Table 5: Models Backpropagation (BP) training hyperparameters, used for training from scratch on original data. AdamW was used as weights optimizer.

Model	Loss	θ_{lr}^*	Weight decay
VGG5	SE	$2.5e^{-4}$	$3e^{-4}$
VGG7	SE	$2.5e^{-4}$	$2e^{-4}$
VGG9	CE	$5e^{-4}$	$3e^{-4}$
MLP	CE	$1e^{-3}$	$1e^{-4}$

* Weights learning rate.

Table 5 reports the hyperparameters that were used to train the models with BP on original data (Figure 4).

Table 6 describes the CNNs training hyperparameters in which the design space exploration took place.

Table 6: Training hyperparameters used for the search of the best model for the Backpropagation (BP) and the Predictive Coding (PC) training.

		PC			
		BP VGG5-7-9	VGG5	VGG7	VGG9
Loss		[SE, CE]	[SE, CE]	[SE, CE]	[SE, CE]
Weights update	θ_{lr}^*	$[1e^{-4}, 2.5e^{-4}, 5e^{-4}, 1e^{-3}\S]$	$[1e^{-4}, 1e^{-3}]$	$[1e^{-4}, 1e^{-3}]$	$[1e^{-4}, 1e^{-3}]$
	Weight decay	$[1, 2, 3]e^{-4}$	$1e^{-4}$	$1e^{-4}$	$1e^{-4}$
Predictions update	γ^\dagger	-	$[1e^{-5}, 1e^{-4}, 1e^{-3}, 1e^{-2}, 2.5e^{-2}, 5e^{-2}]$	$[1e^{-5}, 1e^{-4}, 1e^{-3}, 1e^{-2}, 2.5e^{-2}, 5e^{-2}]$	$[1e^{-5}, 1e^{-4}, 1e^{-3}, 1e^{-2}]$
	m^\ddagger	-	$[0.1, 0.5]$	$[0.1, 0.5]$	$[0.1, 0.5, 0.9]$

* Weights learning rate.

† Inference rate.

‡ SGD optimizer momentum.

§ A weights learning rate (θ_{lr}) of $1e^{-3}$ was used only for BP domain adaptation.

For the PC-based trainings of VGG9, the hyperparameter design space exploration has been focused on higher momentums for the SGD optimizer, instead of focusing on high inference rates. This decision has been taken to explore hyperparameters combinations that would favor the training stability, as VGG9 has been proven to be harder to train with PC.

In order to avoid abrupt changes in the test accuracy for the PC-based trainings, the training hyperparameters choice has been constrained to the ones for which, during the design space exploration, the following properties held:

- After the 5th epoch, there was never a test accuracy decrease of no more than 5 percentage points between one epoch and the next.
- The final epoch accuracy was no lower than 5 points with respect to the maximum one.

Regarding the BP-based domain adaptation, a weights learning rate (θ_{lr}) of $1e^{-3}$ has been used only for this training technique, since lower θ_{lr} values did not always provide a satisfactory test accuracy.

Finally, Table 7 summarizes the epochs, batch size, normalization values and data augmentation that were used for training from scratch and domain adapting, both using BP and PC.

Table 7: Summary of training epochs, batches, normalization values and data augmentations for the datasets used in the experiments.

	MNIST	CIFAR10
Training Epochs	10	100
Batch size	128	128
Normalization mean	-	[0.4914, 0.4822, 0.4465]
Normalization standard deviation	-	[0.2023, 0.1994, 0.2010]
Data augmentation	-	(4, 4) zero pad + random cropping 32x32, random (50%) horizontal flip